Quartz Crystal Microbalance Studies of Biomolecule Binding to Cranberry Derived Proanthocyanidins

By Nicole Weckman

Department of Chemical Engineering

McGill University, Montreal

August 2013

A thesis submitted to McGill University

in partial fulfillment of the requirements of the degree of

Master of Engineering

Abstract

While cranberry consumption has been linked with the prevention of bacterial infections in the urinary tract for many years, our understanding of the bioavailability and mechanisms by which cranberry prevents bacterial infection is limited. Despite frequent use in clinical trials, it is hypothesized that the bioavailability of cranberry derived materials in the urinary tract may be limited due to their interaction with human serum proteins such as albumin, α-1-acid glycoprotein (AAG), and fibrinogen. Upon reaching the urinary tract, cranberry derived materials may interfere with bacterial pathogenesis via interaction with the lipopolysaccharides (LPS) on the bacterial cell surface and the secreted biosurfactant, rhamnolipid. Quartz crystal microbalance with dissipation monitoring (QCM-D) is a sensitive mass sensor that is used in this study to directly investigate the interactions between cranberry derived materials and human serum proteins (albumin, AAG, and fibrinogen) or bacterial components (LPS and rhamnolipid). The binding of cranberry proanthocyanidins (CPAC) to all three serum proteins, the rhamnolipids, and LPS from the uropathogen *Escherichia coli* O111:B4 can be described by Langmuir-type isotherms allowing the determination of the apparent adsorption affinity constant between the CPAC and each biomolecule. CPAC interacts most strongly with fibrinogen with a binding constant of 2.2×10^{8} M^{-1}. CPAC exhibits weaker interactions with albumin and AAG, with binding constants of 2.4×10^{6} M^{-1} and 1.5×10^{6} M^{-1}, respectively. These binding interactions will limit the bioavailability of the CPAC at the site of action thus highlighting the need for an improved understanding of the bioavailability and pharmacokinetics of cranberry consumption before further clinical trials. Furthermore, CPAC interacts with LPS from *Pseudomonas aeruginosa* 10 in a fundamentally different manner than it interacts with *E. coli* O111:B4 LPS or *P. aeruginosa* rhamnolipids, supporting the theory that there are multiple mechanisms via which cranberry prevents bacterial infections and that cranberry may be more effective at preventing certain bacterial infections.

Résumé

Tandis que la consommation de canneberge a été liée à la prévention d'infections bactériennes dans les voies urinaires pendant de nombreuses années, notre compréhension de la biodisponibilité et les mécanismes par lequel canneberge empêche les infections bactériennes est limitée. Malgré l'utilisation fréquente dans les essais cliniques, la biodisponibilité de matières dérivées de canneberges dans les voies urinaires peut être limitée en raison de leur interaction avec les protéines de sérum humain tels que l'albumine, α-1 glycoprotéine acide (AAG) et du fibrinogène. Dès qu'elles arrivent à la voie urinaire, les matières dérivées de canneberges peuvent interférer avec la pathogenèse bactérienne via l'interaction avec les lipopolysaccharides (LPS) sur la surface bactérienne et les biosurfactants sécrétées, rhamnolipide. Microbalance à quartz avec la surveillance de la dissipation (QCM-D) est un instrument capable de détecter de mass avec une haute sensibilité qui est utilisé dans cette étude d'enquêter directement sur les interactions entre les matières dérivées de canneberges et protéines de sérum humain ou des composants bactériens (LPS et rhamnolipide). Les liaisons entre les proanthocyanidines de canneberge (CPAC) et les trois protéines sériques, les rhamnolipides, et le LPS de *Escherichia coli* O111:B4 uropathogènique peut être décrite par les isothermes de type Langmuir permettant la détermination de la constante d'affinité apparente d'adsorption entre la CPAC et chaque biomolécule. CPAC interagit fortement avec le fibrinogène avec une constante de fixation de $2.2x10^{8}$ M^{-1}. CPAC a des interactions plus faibles avec l'albumine et AAG, avec les constantes de fixation de $2.4x10^{6}$ M^{-1} et $1.5x10^{6}$ M^{-1}, respectivement. Ces interactions de liaison limiteront la biodisponibilité de la CPAC au site d'action, mettant ainsi en évidence la nécessité d'une meilleure compréhension de la biodisponibilité et la pharmacocinétique de la consommation de canneberge avant d'autres essais cliniques. De plus, CPAC interagit avec le LPS de *Pseudomonas aeruginosa* 10 de manière fondamentalement différente qu'il interagit avec le LPS de *E. coli*

O111:B4 ou rhamnolipides de *P. aeruginosa*, soutenant la théorie selon laquelle il y a plusieurs mécanismes par laquelle canneberge empêche les infections bactériennes et la canneberge peut-être plus efficace pour prévenir certaines infections bactériennes.

Acknowledgements

The completion of this thesis would not have been possible without the support and assistance of numerous people. First and foremost, I am grateful to my supervisor Professor Nathalie Tufenkji for the opportunity to work in her lab, and for her guidance, and expertise.

Secondly, there are numerous postdoctoral fellows and graduate students in the Biocolloids and Surfaces Research Group who have been exceedingly generous with their technical advice and encouragement. Most particularly, I would like to thank Adam Olsson, Ché O'May, Andreas Wargenau, and Flavio Piccapietra for their ideas, opinions, and knowledge.

Thirdly, thanks to Daniel Dixon, Sarah Decker, and my various office mates for the stories, the moral support, and the much needed coffee breaks. Special thanks to my sister, my parents, and the other members of my extended family for their understanding in stressful times and for never faltering in their belief in me.

This project would not have been possible without financial support from Natural Sciences and Engineering Research Council of Canada, the Canada Research Chairs Program, the Eugenie Ulmer Lamothe Fund at McGill, the Wisconsin Cranberry Board and the Cranberry Institute. Finally, I would also like to thank the Chemical Engineering faculty and staff for their aid throughout my time as a McGill Master's student.

Preface and Contribution of Authors

This thesis is submitted in compliance with the McGill University thesis preparation and submission guidelines and is formatted as a manuscript based thesis. Chapter 1 contains the thesis introduction and objectives. Chapter 2 reports research on the use of the quartz crystal microbalance for the investigation of biomolecule binding to cranberry derived proanthocyanidins and is presented in manuscript form. The manuscript will be submitted to *Langmuir* and authorship of the manuscript will be Nicole Weckman, Adam L.J. Olsson, and Nathalie Tufenkji. Chapter 3 contains the thesis conclusions and recommended future work.

The experimental work, data analysis, and writing of the manuscript was performed by Nicole Weckman. Adam Olsson and Andreas Wargenau provided expertise and experimental support on the QCM-D and ellipsometer, respectively. Adam Olsson and Ché O'May were involved in the experimental design and the editing of the manuscript. Nathalie Tufenkji provided guidance and expertise in a supervisory role throughout the project and in the manuscript revision.

_____

Prof. Nathalie Tufenkji

_____

Dr. Adam Olsson

Table of Contents

Table of Figures

Table of Tables

Chapter 1: Introduction

1.1 Urinary Tract Infections

Despite widespread advances in the understanding of risk factors and prevention measures, the most common bacterial illness in adults remains the urinary tract infection (UTI) [1]. In the United States, UTIs are among the top ten reasons for a visit to the emergency room for women aged 15 and older [2], and cause over 11 million visits to the doctor, costing approximately 3.5 billion dollars annually [3]. At some point during their life, about 50% of women will have a UTI, with a 25% chance of recurrence within 6 months [4].

While *Escherichia coli* is responsible for the majority of cases, other Gram-negative bacteria including *Proteus mirabilis*, and *Pseudomonas aeruginosa* are also associated with UTIs [3]. Once uropathogenic bacteria are present in the urinary tract, they must overcome the host defenses and immune inflammatory response, bactericidal molecules in the urinary tract, and urine flow in order to establish the infection [5]. This process is facilitated by crucial bacterial behaviours and mediated by virulence factors characteristic of uropathogenic bacteria.

1.1.1 Virulence Factors Associated With UTIs

There are many different bacterial behaviours that play a role in the pathogenicity of bacteria in UTIs including bacterial adhesion to host cells, bacterial motility, toxin production, iron acquisition, and evading the immune response of the host [3]. Two key steps in the development and progression of a UTI are bacterial adhesion to host cells [6] and bacterial motility which allows the spreading of the infection from the urinary tract to the bladder or even to the kidney [7]. These steps are mediated by virulence factors expressed by uropathogenic bacteria.

A virulence factor can be defined as a "protein (such as a toxin) or macromolecular structure (such as a fimbria or flagellum) that contributes to the ability of the pathogen to cause disease" [3]. There are many identified virulence factors for bacteria associated with UTIs, including fimbriae that are involved in bacterial adhesion to the host cells [8-10], flagella which mediate bacterial motility [11, 12], and molecules excreted by the bacteria such as extracellular polysaccharides [10]. There exists a plethora of molecules that are involved in bacterial adhesion, bacterial motility, or are excreted by the bacteria that could be potentially important virulence factors for UTIs.

As the primary component of the outer cell membrane of most Gram-negative bacteria, bacterial lipopolysaccharides (LPS) are required for swarming motility [13], and are important to both the structure and the overall surface charge of the bacteria [14]. LPS molecules consist of a hydrophobic lipid A section, a core section, and a long polysaccharide chain known as the O-antigen [15]. The LPS molecule including the long O-antigen can protrude over 30 nm from the cell surface and may contribute significantly to the forces dominating bacterial adhesion [16]. These factors contribute to the importance of LPS as a virulence factor and a cellular adhesion molecule [15]. An example of a LPS molecular structure can be seen in Figure 1 [17]:

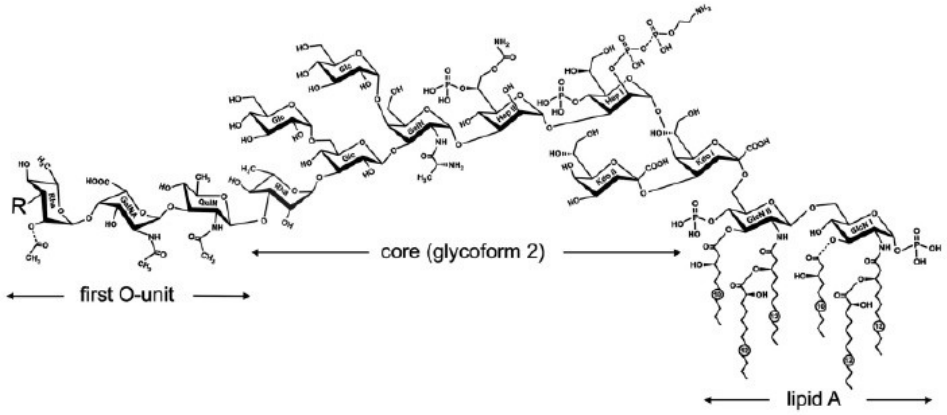

Figure 1: The chemical structure of a *P. aeruginosa* LPS molecule.

Another biomolecule that is considered to be a virulence factor is the biosurfactant rhamnolipid that is produced primarily by the opportunistic bacterium *P. aeruginosa* [18, 19]. Rhamnolipid production is regulated by the *rhl* quorum sensing signaling pathway [20] which has been found to be a virulence factor for *P. aeruginosa* UTIs in animal models [21]. Rhamnolipids also play a key role in bacterial motility; *P. aeruginosa* mutants that are deficient in rhamnolipid production have been shown to have altered swarming patterns [22]. An example of the chemical structure of mono- and di-rhamnolipids can be seen in Figure 2 [23]:

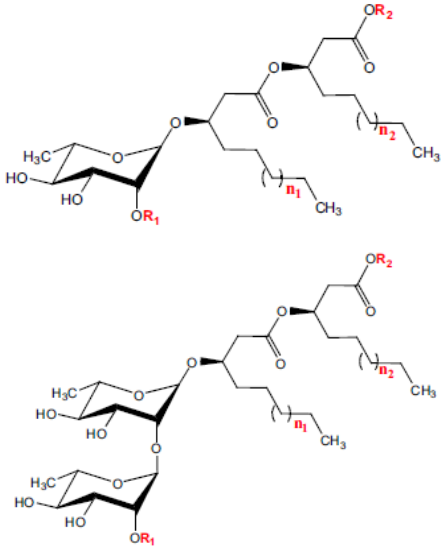

Figure 2: An example of the chemical structure of mono- and di-rhamnolipids.

Because of their known role as virulence factors for a variety of diseases and their contribution to bacterial adhesion and motility, both LPS and rhamnolipids are quite likely to play a role in the virulence of uropathogenic bacteria.

1.1.2 Traditional Treatment of Recurrent UTIs

The recommended treatment for acute uncomplicated UTIs is from one day to about a week of antibiotics [1]. However, only 5 days of treatment with ciprofloxacin, a fluoroquinolone antibiotic, has been shown to affect the abundance of about one third of the bacteria in the gut, in some cases taking months to return to normal [24]. Even worse than the short treatment for an acute infection, recurrent UTIs are traditionally treated with a low dose prophylactic antibiotic regime, a treatment that is strongly associated with the development of antibiotic resistant bacteria [25]. Antibiotic resistant uropathogens are increasingly common worldwide, leading to the need for non-antibiotic therapeutic and preventative approaches to UTIs [1, 4].

1.2 North American Cranberry Proanthocyanidins

The North American cranberry, or *Vaccinium macrocarpon*, has been found to have many beneficial effects on human health, ranging from prevention of cardiovascular diseases and cancers due to antimutagenic and antioxidant properties, to the ability to modify bacteria behaviour, interfering with virulence factors and leading to the prevention of common bacterial infections [26]. Specifically, cranberry consumption, primarily in the form of cranberry juice, has been associated with the prevention of urinary tract infections for nearly a century [27]. While there are many suspected biologically active compounds in cranberries, including anthocyanins, phenolic acid derivatives, and the monosaccharide fructose, it is the cranberry proanthocyanidins (CPAC), that are most commonly believed to be the fraction that plays an important role in bacteria-cell interactions [27-29].

Proanthocyanidins are polyphenolic compounds that are produced by plants when experiencing environmental stress or microbial infection [27]. They are condensed tannins composed of the flavonoid subunits catechin and epicatechin

[30], with a degree of polymerization of 4-5 shown to be most effective for the inhibition of bacterial adhesion to uroepithelial cells [31]. The activity of CPACs has been shown to be related not only to the size of the polymer, but also to the type of bond between the subunits, an A-type linkage or a B-type linkage [27]. The linkages can be compared in the figure below showing a tetramer with 2 B-type linkages and one A-type linkage [29, 32]:

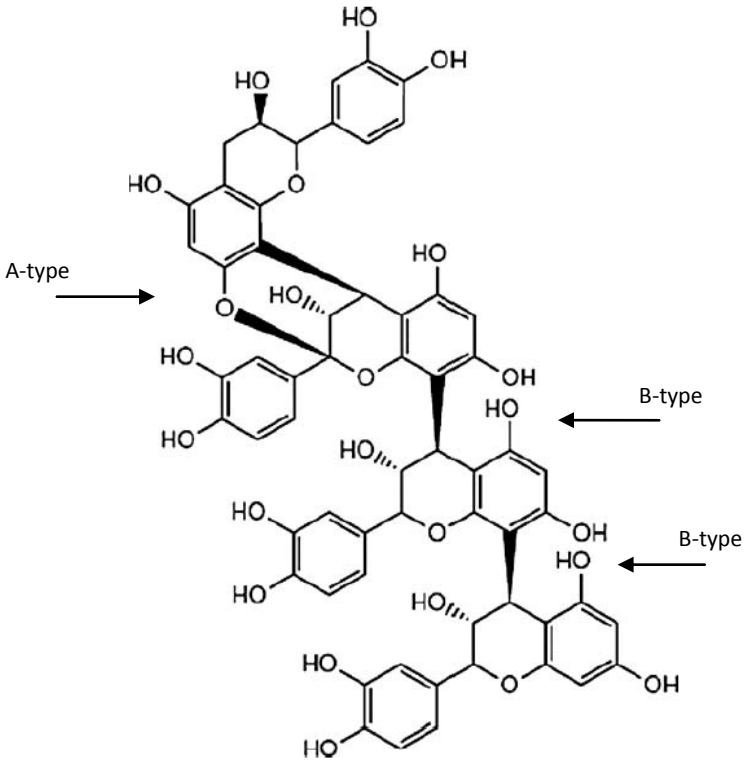

Figure 3: The chemical structure of a proanthocyanidin tetramer containing one highlighted A-type linkage and 2 highlighted B-type linkages.

CPAC activity is associated with at least one A-type linkage between subunits [31]; as shown in Figure 3 above, an A-type linkage is composed of both a carbon-carbon single bond and an ether carbon-oxygen bond between the subunits, rather than the more common B-type linkage consisting of only the carbon-carbon single bond [33].

1.2.1 Mechanisms of CPAC Action

Historically, it was believed that the main mechanism via which consumption of cranberry prevented UTIs was through changing the acidity of urine [34], however recent studies have shown that the consumption of cranberry capsules or juice does not consistently increase the acidity of urine [35, 36]. Thus, research has increasingly focused on other potential mechanisms of cranberry action.

It has been proposed that one possible mechanism by which cranberry prevents bacterial infections is by impairing bacterial adhesion to host cells, a critical step in the development of bacterial infections [37]. Several possibilities for the mechanism involved in the inhibition of bacterial adhesion due to cranberry treatment have been proposed, including cranberry induced alteration of bacterial surface properties [38, 39], cranberry induced alteration of bacterial morphology and shape [40], CPAC interference with P-type fimbriae of *Escherichia coli* [41], and CPAC induced actin cytoskeleton rearrangement of host cells that reduces formation of focal adhesion points or pedestals necessary for bacteria-cell interaction [42].

There have been multiple recent studies on the effects of cranberry derivatives on bacterial adhesion to biomaterials and cells. Cranberry extract has been shown to reduce the attachment strength and non-specific binding of *E. coli* to a glass substrate [43, 44], to reduce *E. coli* adhesion to silicone rubber [35] and to the common biomaterials poly(vinyl chloride) (PVC) and polytetrafluoroethylene (PTFE) [28]. CPACs have also been shown to decrease the adhesion of bacteria to epithelial cell receptors [31] and to primary cultured bladder cells [45]. Finally, urine collected after cranberry consumption has been shown to decrease the adhesion forces of bacteria as measured by an AFM probe [46] and to decrease adhesion of bacteria to uroepithelial cells [47].

Another mechanism via which cranberry interferes with bacterial virulence is through decreasing the motility of the bacteria. CPAC has been shown to completely block the swarming motility of *P. aeruginosa*, although this motility is partially restored upon the addition of rhamnolipids [30]. CPAC also inhibits the expression of the flagellin gene thereby impairing swimming and swarming motilities of uropathogenic *E. coli* [48] and *Proteus mirabilis* [49].

Two final mechanisms via which cranberry could decrease bacterial virulence is through interference with bacterial iron acquisition and interactions with the immune response of the host; CPACs have been shown to induce a state of iron limitation on uropathogenic *E. coli* [50] and to bind to the cell membrane lipopolysaccharides (LPS) of multiple bacteria, inhibiting their interaction with cells by blocking the LPS-TLR4/MD2 interaction [33].

1.2.2 CPAC Bioavailability

Because of the increasing evidence supporting the ability of cranberry to decrease bacterial virulence *in vitro*, clinical trials into the efficacy of cranberry as a preventative measure against recurrent UTIs have become more common. Although numerous clinical studies have been recently performed, their results have been conflicting, with certain studies showing a reduction in recurrence of UTIs [51] and others showing no reduction [52] as compared to a control group. This could be due to the fact that the bioavailability and metabolic fate of cranberry derived materials from the time of ingestion to urinary excretion is not well understood [53, 54].

There are many factors that play a role in the bioavailability of a drug at the desired site of action. In the case of CPAC consumption for the treatment of UTIs, the CPAC must be absorbed by the gut into circulation and then excreted into the urine. Absorption is not guaranteed as certain studies show that as the molecular weight of proanthocyanidins increases, absorption through the gut barrier decreases [55]. Once absorbed, the molecules would be further

metabolised by the liver before entering general circulation in the blood stream [56]. Once in the blood, a common factor that can limit the bioavailability of a drug at the site of action is drug binding to plasma proteins such as human serum albumin (HSA), fibrinogen, and α-1-acid glycoprotein (AAG). Only unbound drug is free to reach the active site [57]; hence, the binding of cranberry derivatives such as CPAC to serum proteins may limit their bioavailability in the urinary tract. A few studies have been done on the binding of proanthocyanidins and tannins to model proteins like bovine serum albumin and selected proteins in the intestine or saliva [53, 58-60], however no study has systematically investigated the binding of CPACs to important plasma proteins.

1.3 Quartz Crystal Microbalance with Dissipation Monitoring

1.3.1 Theory and Development of the Quartz Crystal Microbalance (QCM)

While piezoelectric material properties have been understood since the late 19th century, the development and use of the quartz crystal microbalance (QCM) taking advantage of the unique quartz piezoelectric material properties for mass measurements precise to less than a nanogram is relatively recent [61]. The QCM is based on quartz piezoelectric properties; an applied AC voltage oscillating at approximately the QCM resonant frequency induces an oscillating expansion and contraction of the crystal lattice [62]. In the case of the QCM, a minute change in the mass on the quartz crystal surface is sufficient to affect the crystal oscillation and thus cause a detectable resonant frequency shift. The field concerning the use of the QCM to investigate adsorption and deposition phenomena emerged after the investigations of Sauerbrey led to his 1959 study reporting what has now become known as the Sauerbrey equation [62-64]. The Sauerbrey equation describes the linear relationship between shifts in the resonant frequency of a quartz crystal to changes in mass on the crystal surface [62, 64]:

$$\Delta f = -\frac{nf_0}{t_q \rho_q} \Delta m = -\frac{n}{C} \Delta m$$

where Δf is the observed frequency shift in Hz, Δm is the change in mass at the crystal surface in ngcm^{-2}, t_q is the thickness of the quartz crystal, ρ_q is the density of quartz, f_0 is the resonant frequency of the crystal in Hz, n is the odd overtone number, and C is generally 17.7 ngcm^{-2}Hz^{-1} for a 5 MHz crystal. Based on the assumptions made in the derivation of the Sauerbrey equation, it is limited to rigidly attached homogeneous thin films growing at the crystal surface [62]. Due to Sauerbrey's developments, investigations into such phenomena as vacuum deposition, observation of stress effects, oxide growth on metal surfaces, gas phase detection of compounds like hydrocarbons, and gas absorption on surfaces proceeded [62, 65, 66], however QCM application to systems involving liquid, including biological systems, was still limited. Biological systems could only be studied using QCM following several advances in the 1980s, including the development of oscillator circuits that can function efficiently in liquid [67], and several extensions to the Sauerbrey equation describing both the frequency shift of a submerged crystal due solely to the effects of the density and viscosity of the liquid [68], and the frequency shift due to combined rigid mass deposition and the effects of the liquid medium [69].

An additional QCM advance significant to exploration of biological systems was the development of quartz crystal microbalance with dissipation monitoring, QCM-D, allowing dissipation monitoring concurrently with the monitoring of frequency shifts. The dissipation of a crystal is mathematically defined as [62]:

$$D = \frac{1}{Q} = \frac{E_{dissipated}}{2\pi E_{stored}}$$

where D is the dissipation and is dimensionless, Q is the quality factor, and E is the energy being either dissipated or stored during one oscillation of the crystal

system. The dissipation is measured by rapidly driving the crystal near the resonance frequency and then observing the decay in the oscillation over time, a technology first presented by Rodahl et al. in 1995 and commercialized by the company Q-Sense [62, 70].

Whereas small and rigid molecule adsorption requires only monitoring of frequency shifts and analysis using the Sauerbrey equation, larger more flexible molecule adsorption or the adsorption of molecules coupled with water require dissipation monitoring for accurate analysis [61, 62]. Furthermore, the real time analysis of both the frequency and the dissipation concurrently allow the investigation of the effects on the viscoelastic properties of an adsorbed layer due to changes in ionic strength or pH [71, 72], temperature [73], polymerization [74, 75], or even complex processes such as blood clotting [76]. The combination of the measurement of the mass change on the crystal surface based on frequency shifts, and the measurement of the viscoelastic properties of the surface layers based on the energy dissipation shifts, provides a powerful tool for the analysis of biological systems.

1.3.2 Biological Applications of the QCM and QCM-D

Many biological systems have been investigated using either QCM or QCM-D. They have been used to study various properties of DNA, whether to analyze the size and conformation of the DNA itself [77], monitor damage to DNA exposed to a toxin [78], or create a DNA biosensor [79]. Lipids, carbohydrates like cellulose and polysaccharides, small molecules such as insecticides or cyanides, heavy metal ions, viruses, and phage are all examples of other biological compounds that have been studied or detected using QCM and QCM-D technology [61-63]. However, perhaps the area of highest interest in QCM applications is protein adsorption, with particular attention being paid to the investigation of protein adsorption to biomaterials [80-84], and protein-protein interactions, often targeted towards antibody-antigen immunosensors [85-87].

1.4 Objectives

The objective of this thesis was to use the QCM-D to directly investigate the interactions between CPAC and biomolecules in real-time. The research was performed to test the hypothesis that CPAC interferes with bacterial pathogenesis via interaction with the virulence factors LPS, found on the bacterial cell surface, and rhamnolipid, the secreted biosurfactant, and to elucidate potential interactions with serum proteins that could limit bioavailability of CPAC at infection sites. Specifically, the QCM-D was used to:

1. Investigate interactions between CPAC and LPS from the uropathogens *E. coli* O111:B4 and *P. aeruginosa* 10

2. Investigate interactions between CPAC and rhamnolipids from *P. aeruginosa*

3. Investigate interactions between CPAC and albumin, fibrinogen, and AAG found in human serum

Chapter 2: Quartz Crystal Microbalance Studies of Biomolecule Binding to Cranberry Derived Proanthocyanidins

2.1 Introduction

The North American cranberry, or *Vaccinium macrocarpon*, has been found to have many beneficial effects on human health including the ability to modify bacteria behaviour, reduce virulence and prevent selected common bacterial infections [26]. Specifically, cranberry consumption, primarily in the form of cranberry juice, has been associated for almost a century with the prevention of urinary tract infections (UTIs) [27]. Recurrent UTIs are traditionally treated with a low dose antibiotic regime, a treatment that is strongly associated with the development of antibiotic resistant bacteria [25]. While cranberry, in particular the cranberry proanthocyanidin (CPAC) fraction, has been increasingly researched as a natural and widely available alternative to traditional antibiotic regimes for the prevention of recurrent UTIs, our understanding of the bioavailability and the mechanisms by which cranberry prevents bacterial infection is limited.

Although numerous clinical studies have been performed investigating the consumption of cranberry to prevent recurrent UTIs, the bioavailability and metabolic fate of cranberry derived materials from the time of ingestion to urinary excretion is not well understood [53, 54]. A common factor that can limit the bioavailability of a drug at the site of action is drug binding to plasma proteins such as human serum albumin (HSA), fibrinogen, and α-1-acid glycoprotein (AAG). Only unbound drug is free to reach the active site [57]; hence, the binding of cranberry derivatives such as CPAC to serum proteins may limit their bioavailability in the urinary tract. While a few studies have been done on the binding of proanthocyanidins to model proteins like bovine serum

albumin and selected proteins in the intestine [53, 58, 59], it is important to investigate the binding of CPACs to human serum proteins, such as HSA, fibrinogen, and AAG, that could functionally affect CPAC bioavailability.

In addition to uncertainty in the bioavailability of CPAC, the mechanism by which it prevents bacterial infections is not entirely understood. Two key steps in the development and progression of a UTI are bacterial adhesion to host cells and bacterial motility which allows the spreading of the infection from the urinary tract to the bladder or even to the kidney [3]. It has been proposed that one possible mechanism by which cranberry prevents bacterial infections is by impairing bacterial adhesion to host cells, a critical step in the development of bacterial infections [37]. Several possibilities for the mechanism involved in the inhibition of bacterial adhesion due to cranberry treatment have been proposed, including cranberry induced alteration of bacterial surface properties [38], cranberry induced alteration of bacterial morphology and shape [40], and CPAC interference with P-type fimbriae of *Escherichia coli* [41]. Another mechanism via which CPAC interferes with bacterial virulence is through decreasing the motility of the bacteria. CPAC has been shown to completely block the swarming motility of *Pseudomonas aeruginosa* [30] and to inhibit the expression of the flagellin gene thereby impairing swimming and swarming motilities of uropathogenic *E. coli* [48] and *Proteus mirabilis* [49].

As the primary component of the outer cell membrane of most Gram-negative bacteria, including the aforementioned pathogens associated with UTIs, bacterial lipopolysaccharides (LPS) are required for swarming motility [13], and are important to both the structure and the overall surface charge of the bacteria [14]. These factors contribute to the importance of LPS as a virulence factor and a cellular adhesion molecule [15]. As such, the binding of CPAC to LPS could play a role in the inhibition of bacterial adhesion *in vivo*. LPS molecules consist of a hydrophobic lipid A section, a core section, and a long polysaccharide chain

known as the O-antigen [15]. When LPS from various bacteria is present at low concentrations in solution, CPACs have been shown to bind to the highly conserved lipid A portion of the molecule [33]. However, in aqueous solution at concentrations greater than the critical micelle concentration, LPS forms micelles with the hydrophobic lipid A group anchored in the micelle and the O-antigen projecting into the medium, a structure more representative of the natural molecular conformation in the bacterial outer membrane [88]. Thus, to investigate the potential mechanisms by which CPAC may inhibit bacterial adhesion, it is of interest to examine the binding interactions between CPAC and LPS micelles.

Another biomolecule that is considered to be a virulence factor and to play a key role in bacterial motility is the biosurfactant rhamnolipid, produced by the opportunistic bacterium *P. aeruginosa* [18, 19]. Rhamnolipid production is regulated by the *rhl* quorum sensing signaling pathway [20] and has been found to be a virulence factor for *P. aeruginosa* UTIs in animal models [21]. Furthermore, *P. aeruginosa* mutants that are deficient in rhamnolipid production have been shown to have altered swarming patterns [22]. While the presence of CPAC inhibits *P. aeruginosa* swarming motility, addition of rhamnolipid has been found to partially restore motility [30]. Thus, interaction between CPAC and rhamnolipid is one possible mechanism via which CPAC inhibits bacterial motility, and is worthy of further investigation.

A useful technique for the measurement of molecular interactions such as the binding of CPAC with various biomolecules is the quartz crystal microbalance with dissipation monitoring, or QCM-D. The QCM-D is a mass sensor with nanogram sensitivity that allows real-time quantitative analysis of biomolecule adsorption and interactions [75]. The study of biological interactions is an area of high interest in QCM applications and has been thoroughly reviewed elsewhere [61, 62]. Particularly, the use of the QCM for quantification of protein

interactions with surfaces, other proteins, and small molecules has been demonstrated [85, 86, 89, 90]. Moreover, a previous study has shown that QCM-D can be useful for measuring adsorption of CPAC onto materials used in the manufacture of urinary catheters (PVC and PTFE) [28]. Thus, QCM-D can be a useful tool to directly investigate and quantify the binding interactions between CPAC and human serum proteins, LPS, and rhamnolipid.

The purpose of this study is two-fold: (i) to evaluate potential limitations to the bioavailability of a cranberry derivative, namely, CPAC, by characterizing its extent of binding to human serum proteins, and (ii) to investigate the potential interfering role of CPAC against selected bacterial virulence factors (LPS and rhamnolipids) by measuring their extent of binding to CPAC. A QCM-D is used to measure adsorption of three different human serum proteins (HSA, fibrinogen, and AAG) to a layer of CPAC formed on the surface of the sensor. The same approach is used to quantify binding of LPS from two different uropathogens (*E. coli* O111:B4 and *P. aeruginosa* 10) as well as rhamnolipids from *P. aeruginosa* to CPAC. After demonstrating that all of these biomolecules bind to the CPAC coated surface, the Langmuir adsorption model is used to calculate relative binding affinities of the molecules for CPAC and other adsorption and thermodynamic parameters.

2.2 Materials and Methods

2.2.1 Solutions

Phosphate buffered saline (PBS) solution was prepared by dissolving a PBS tablet (Sigma-Aldrich) in deionized (DI) water and was filtered using a 0.22 μm membrane to remove impurities.

Dry cranberry proanthocyanidin (CPAC) powder isolated from *Vaccinium macrocarpon* (obtained from A.B. Howell, Rutgers, Chatsworth, USA) was dissolved in DI water at a concentration of 1mg/mL to form a stock solution. This

stock solution was filtered through a 0.22 µm membrane to remove impurities, and was stored at 4°C protected from light. The stock solution was diluted to a concentration of 100 µg/mL in PBS as needed.

LPS from *Escherichia coli* O111:B4 (ELPS) and *Pseudomonas aeruginosa* 10 (PLPS), as well as HSA, fibrinogen, and AAG from human serum, were purchased from Sigma-Aldrich and dissolved in PBS to form stock solutions with a concentration of 1 mg/mL. The molecular weights assumed for the ELPS, PLPS, HSA, fibrinogen, and AAG were 10 kDa, 10 kDa, 66 kDa, 340kDa, and 40.8 kDa, respectively, as listed in the Sigma product sheets. The stock solutions of LPS and proteins were stored at 4°C and kept for no longer than 1 week. R95 rhamnolipids (AGAE Technologies, LLC, Corvallis, USA) were stored as a stock solution of 61.2 µg/mL at 4°C until needed. The rhamnolipids are a mixture of mono- and di-rhamnolipid in a ratio of about 1:5, and an average molecular weight of 626 g/mol is assumed. Stock solutions were diluted in PBS to the desired concentration before each experiment.

2.2.2 Quartz Crystal Microbalance with Dissipation Monitoring

All QCM-D experiments were performed in an E4 QCM-D unit from Q-Sense (Q-Sense AB, Göteborg, Sweden) using purchased AT-cut quartz crystals coated with titanium (QSX310) with a fundamental resonance frequency of 5MHz. Titanium coated crystals were chosen as a model surface due to consistent and significant CPAC adsorption to the surface. Prior to each experiment, the crystals were cleaned by soaking in a 2% Hellmanex solution for at least 30min. They were then sonicated for 10 minutes in the 2% Hellmanex solution before being thoroughly rinsed with DI water and dried with nitrogen gas. Finally, the crystals were exposed to ultraviolet light for 20min immediately before the experiment.

A peristaltic pump (RegloDigital, Ismatec) was used to maintain the flow at negative pressure through the QCM-D modules at 150 µL/min for all experiments. The temperature was maintained at 22 °C throughout the

experiments using the built in temperature controller of the QCM-D. Frequency and dissipation baselines in DI water and in PBS were allowed to stabilize before beginning each experiment.

After the establishment of a baseline in PBS, a CPAC solution was flowed at a concentration of 100 µg/mL across the crystal surface in order to deposit a layer of CPAC on the crystal. This was followed by a 10 min rinse with PBS to remove any CPAC that was loosely bound to the crystal surface. The desired LPS, rhamnolipid, or protein solution was flowed across the CPAC coated crystal until the deposition had reached equilibrium. Loosely bound molecules were again rinsed away with a PBS rinse of at least 10 min.

Following each experiment, the QCM-D setup was cleaned by flowing first a 2% Hellmanex solution followed by DI water through the apparatus for at least 10 min each. The water was purged from the modules and tubing using air and nitrogen gas.

2.2.3 Determination of Biomolecule Binding Constants

The QCM is based on quartz piezoelectric properties; an AC voltage applied across two gold electrodes on the quartz crystal induces an oscillating expansion and contraction of the crystal lattice at its resonant frequency or odd overtones thereof [62]. In the case of the QCM, a minute change in the mass on the quartz crystal surface is sufficient to affect the crystal oscillation and thus cause a detectable resonant frequency shift. In 1959, Sauerbrey reported what has now become known as the Sauerbrey equation describing the linear relationship between changes in mass on the crystal surface and shifts in the resonant frequency of a quartz crystal [62, 64]:

$$\Delta m = -\frac{C}{n}\Delta f$$

where Δm is the change in mass at the crystal surface in ngcm^{-2}, Δf is the observed frequency shift in Hz, C is the mass sensitivity constant (C=17.7 ngcm^{-2}Hz^{-1} for a 5 MHz crystal), and n is the odd overtone number, where n=3 was used for all calculations. In quartz crystal microbalance with dissipation monitoring, QCM-D, the energy dissipation is measured concurrently with frequency shifts. The dissipation of a crystal is deduced from the oscillation decay time and is mathematically defined as [62]:

$$D = \frac{E_{dissipated}}{2\pi E_{stored}}$$

where D is the dimensionless dissipation factor, and E is the energy being either dissipated or stored during one oscillation of the crystal system. Traditionally, the Sauerbrey equation is limited to rigid thin films growing at the crystal surface, precluding the study of liquid based biosystems. However, in this case, because the energy dissipation is sufficiently small in all experiments, that is, the $\Delta D/\Delta f$ values are less than 4×10^{-7} Hz^{-1}, the Sauerbrey equation can be used to calculate the mass, and thus the surface concentration, of the biomolecules adsorbed to the CPAC coated crystal surface [91].

The equilibrium surface concentration of the biomolecule bound to the CPAC coated surface can be calculated from the QCM-D mass using the molecular weight of the molecule as listed above. Often the equilibrium surface concentration of an adsorbed biomolecule can be related to the biomolecule concentration in solution using the Langmuir adsorption isotherm [90]:

$$\Gamma = \frac{\Gamma_{max} K C}{1 + KC}$$

where C is the biomolecule solution concentration in mol/L, Γ is the surface concentration of biomolecules in mol/cm^2, Γ_{max} is the maximum surface concentration of a monolayer of biomolecules in mol/cm^2, and K is the binding

affinity constant for the biomolecule-CPAC interaction in L/mol. The isotherm above can be linearized in the following manner [92]:

$$\frac{C}{\Gamma} = \frac{1}{\Gamma_{max} K} + \frac{C}{\Gamma_{max}}$$

By plotting C/Γ versus C and fitting a straight line to the data, the maximum surface concentration and the thermodynamic binding affinity constant can be calculated from the slope and intercept. Furthermore, the binding affinity constant, K, can be used to calculate the apparent Gibbs free energy of adsorption using the following equation [92]:

$$K = \frac{1}{c_{solvent}} \exp\left(\frac{-\Delta G_{ads}}{RT}\right)$$

where K is the binding affinity constant for the biomolecule-CPAC interaction in L/mol, $c_{solvent}$ is the molar concentration of the solvent (assumed to be c_{water}=55.5 molm^{-3}), R is the gas constant in Jmol^{-1}K^{-1}, T is the temperature in K, and ΔG_{ads} is the Gibbs free energy of adsorption in Jmol^{-1}. While providing valuable information on biomolecule binding to the CPAC, the Langmuir isotherm must be used with caution as it depends on several assumptions: reversible adsorption, no lateral interactions on the surface, equal energy of all surface adsorption sites, and monolayer adsorption. Although several of these assumptions have been questioned in the case of protein adsorption, in this case, the Langmuir model is used simply for comparison purposes between the different biomolecules. To limit inaccuracies in the Langmuir adsorption isotherm model due to protein spreading and enable comparison of the binding constants of the various biomolecules, direct QCM-D adsorption measurements for each protein concentration were used rather than sequential QCM-D measurements [90].

2.3 Results and Discussion

2.3.1 Biomolecule Binding to a CPAC Coated Surface Monitored by QCM-D

The CPAC binds to the QCM-D crystal surface causing a negative frequency shift as mass adsorbs, as predicted by the Sauerbrey equation. Upon rinsing the CPAC coated surface with buffer, no desorption is observed indicating a stable CPAC surface coating. The frequency shift of a typical QCM-D experiment involving the adsorption of CPAC, a rinse in buffer, the adsorption of a protein to the CPAC layer, and a final rinse can be seen in Figure 4.

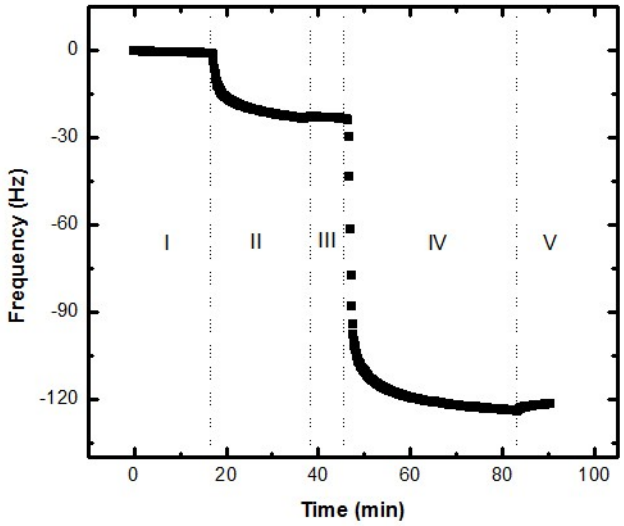

Figure 4: An example of the adsorption of the CPAC coating to the crystal and the subsequent adsorption behaviour of fibrinogen to the CPAC coated surface. Five phases can be seen in the plot: I- Baseline in PBS buffer, II-Adsorption of the CPAC layer, III-Rinse of the CPAC layer with PBS buffer, IV-Adsorption of fibrinogen from a 1.5µM solution causing a negative frequency shift, V-Rinse of the fibrinogen layer with PBS buffer.

As exemplified in Figure 4, all of the biomolecules bind to the CPAC coated surface, causing a negative frequency shift proportional to the adsorbed mass. However, the molecules exhibit vastly different time-dependent adsorption behaviours, examples of which can be seen in Figure 5:

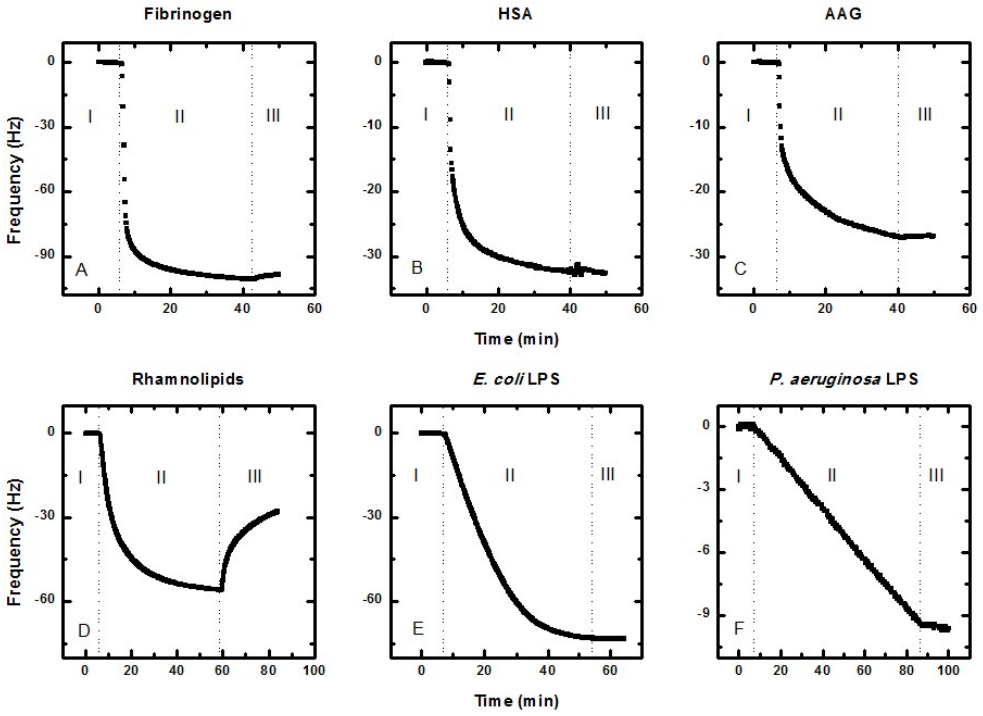

Figure 5: Examples of the time dependent adsorption behaviours of the different biomolecules to the CPAC coated surface. The frequency is normalized to the PBS rinse after CPAC deposition, so three phases can be seen in the plots: I-Rinse of the CPAC layer with PBS buffer, II- Adsorption of the biomolecule from solution causing a negative frequency shift, III-Rinse of the biomolecule layer with PBS buffer. The adsorption from 1.5 µM solutions of (A) fibrinogen, (B) HSA, and (C) AAG and from 10 µg/mL solutions of (D) rhamnolipids, (E) ELPS, and (F) PLPS to the CPAC layer are shown.

For the proteins (Figure 5A-C), the initial rate of adsorption to CPAC is high and the rate of adsorption gradually decreases until an equilibrium surface concentration is reached, at which point the frequency shift remains constant with time. Upon rinsing with buffer once equilibrium adsorption is reached, the frequency for HSA and AAG remains relatively constant at the equilibrium value, indicating that the molecules are tightly bound to the CPAC and exhibit little desorption (Figure 5B-C). In contrast, for the rhamnolipids, the frequency increases from its equilibrium value upon injection of the final PBS rinse, indicating that some molecules are desorbing (Figure 5D). Fibrinogen has two distinct desorption regimes based on initial fibrinogen concentration in solution. At low concentrations, fibrinogen behaves similarly to the other proteins and

only minimal desorption occurs upon rinsing with buffer (Figure 5A), but at high concentrations there is significant desorption during the rinse (data not shown). It is suspected that this occurs because interactions or aggregation of fibrinogen molecules in solution at high concentrations cause the fibrinogen to adsorb to the CPAC in a different orientation with a weaker binding interaction.

While the LPS molecules isolated from *E. coli* and *P. aeruginosa* both bind to the CPAC (Figure 5E-F), they exhibit vastly different binding behaviour. ELPS binds more rapidly to CPAC than PLPS, displaying behaviour similar to the HSA and AAG proteins (Figure 5E). It reaches an equilibrium surface concentration and has little desorption upon rinsing with buffer. The PLPS exhibits completely different time dependent adsorption behaviour from the other molecules investigated. While PLPS binds to the CPAC, it binds at a very slow constant rate and has a much smaller frequency shift over the course of the experiment than the other molecules. Further, it does not appear to reach an equilibrium surface concentration in the typical 2 hour timescale investigated for these experiments (Figure 5F). Similar behaviour is also observed during trial experiments where PLPS is allowed to adsorb to the CPAC overnight, with no equilibrium being reached despite the longer timescale (not shown). Upon rinsing with buffer, the frequency remains constant at the frequency at which buffer was injected, indicating that there is little desorption of the adsorbed PLPS. Because the binding of the PLPS is not observed to reach an equilibrium surface concentration, it is believed that multilayer binding is occurring with the first layer of PLPS binding to the CPAC and further layers binding to previously adsorbed PLPS.

The adsorption behavior of all molecules to the CPAC coated surface is within the Sauerbrey regime [91], allowing the direct calculation of adsorbed mass and thus surface concentration. The ratio of $\Delta D/\Delta f$ at equilibrium adsorption can be used as an indication of the viscoelasticity of the equilibrium layer; this ratio is

calculated for all adsorbed molecules except for PLPS, which never reached equilibrium. The Δ*D*/Δ*f* ratio for the proteins can be seen in Figure 6.

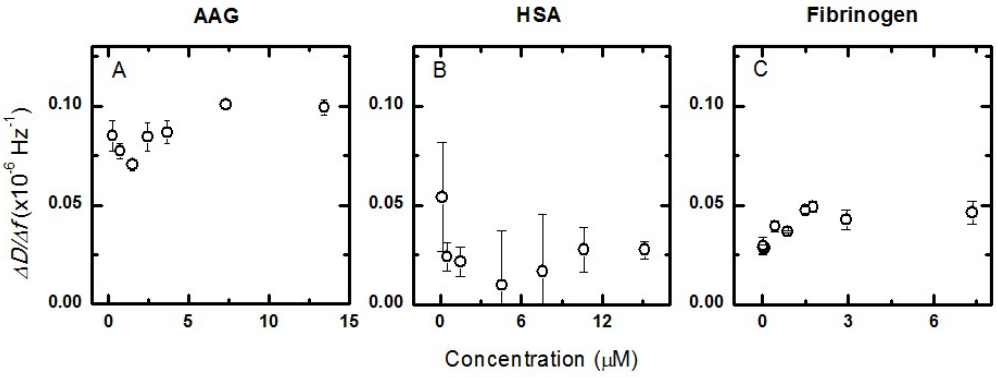

Figure 6: Equilibrium Δ*D*/Δ*f* values calculated at different initial solution concentrations of (A) AAG, (B) HSA, and (C) fibrinogen. All three proteins show relatively low and constant Δ*D*/Δ*f* ratios.

For the proteins, the ratio of Δ*D*/Δ*f* at equilibrium adsorption remains fairly constant across all solution concentrations of protein investigated. This indicates that there is no major change in rigidity or trapped water in the adsorbed layer based on the initial concentration of protein in solution [86].

The Δ*D*/Δ*f* ratios of ELPS and rhamnolipid display distinctly different behaviour than that of the proteins (Figure 7). The Δ*D*/Δ*f* ratio of the ELPS equilibrium adsorption was higher than that of the proteins at all initial concentrations of ELPS in solution (Figure 7A). A higher Δ*D*/Δ*f* ratio is typical of flexible, highly hydrated layers [71]. Thus a higher Δ*D*/Δ*f* ratio is expected for a layer of ELPS molecules with long hydrophilic O-antigen chains that can carry and trap water molecules as they adsorb to the CPAC. The rhamnolipid has two distinct Δ*D*/Δ*f* regimes (Figure 7B). At low concentrations of rhamnolipid in solution, the Δ*D*/Δ*f* ratio is quite low and comparable to the Δ*D*/Δ*f* ratio of the proteins. However, at high rhamnolipid concentrations, despite rhamnolipid being a comparatively small molecule, the Δ*D*/Δ*f* ratio shows a marked increase and approaches that of the ELPS.

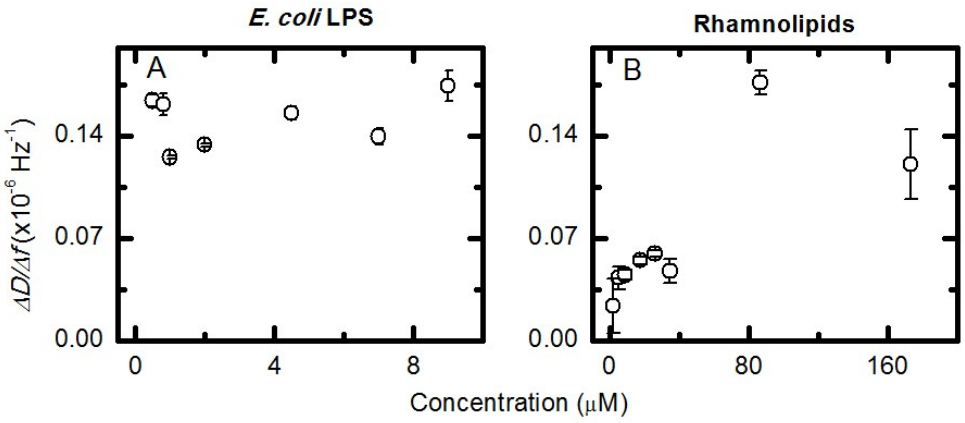

Figure 7: Equilibrium Δ*D*/Δ*f* values calculated at different initial solution concentrations of (A) ELPS and (B) rhamnolipid. The ELPS shows a high, but relatively constant Δ*D*/Δ*f* ratio. The rhamnolipid shows a marked increase in Δ*D*/Δ*f* ratio above the critical micelle concentration.

The adsorption behaviour of the ELPS and rhamnolipid must be analyzed taking into account the amphiphilic nature of these molecules. Both ELPS and rhamnolipids form micelles at concentrations above a critical micelle concentration (CMC) of 22 µg/mL [88, 93], or a molar concentration of about 2.2 µM for ELPS and 35 µM for rhamnolipids. The CMC of the rhamnolipid occurs at a concentration between the adsorption regime with a low Δ*D*/Δ*f* and the adsorption regime with a high Δ*D*/Δ*f*, suggesting a change in adsorbed species from small rhamnolipid molecules to large viscoelastic rhamnolipid micelles. However, for the ELPS, the Δ*D*/Δ*f* ratio remains relatively constant for concentrations both above and below the CMC. This suggests that there is no change in the size or hydration of the binding species, that is, the micelles are not binding to the CPAC coated surface. This result supports the theory that CPAC binds primarily to the lipid A portion of LPS [33]; when the LPS is in micelle form it will not bind to the CPAC because the lipid A is embedded in the hydrophobic core of the micelle rendering it inaccessible. However, more rigorous experimentation is needed to completely rule out CPAC binding to LPS in micellar form, as other explanations exist for the micelles not binding such as

mass transport effects or steric repulsion of the micelles by LPS molecules already bound to the CPAC coated surface.

2.3.2 Langmuir Adsorption Isotherms

The adsorption isotherms of the three proteins, the rhamnolipid, and the ELPS to the CPAC portray characteristic Langmuir adsorption behaviour and can be well described by the linearized Langmuir adsorption models, as exemplified by the fibrinogen isotherms (Figure 8).

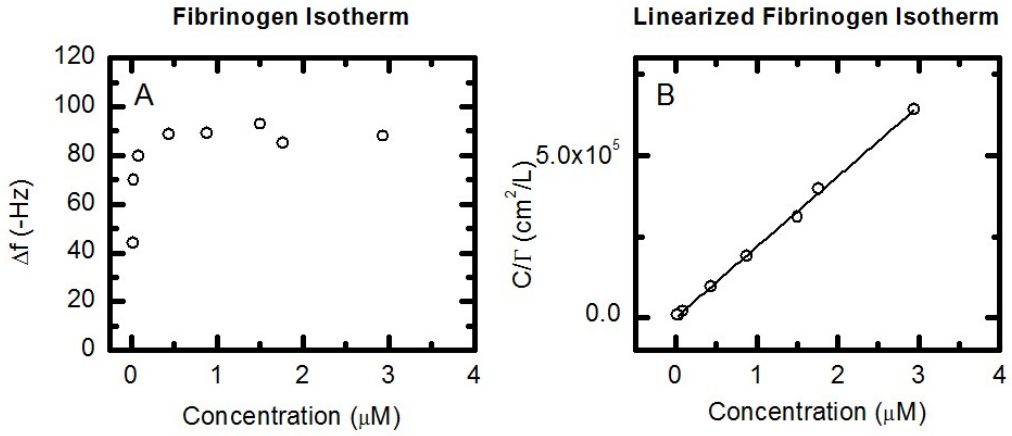

Figure 8: (A) The fibrinogen isotherm showing the frequency shift at equilibrium surface concentration of fibrinogen versus the initial fibrinogen concentration in solution, displays typical Langmuirian behaviour. (B) The linearized Langmuir isotherm for fibrinogen.

The representative isotherm (Figure 8A) shows that the amount of fibrinogen adsorbed to the CPAC at equilibrium increases as the concentration of fibrinogen in solution increases, until it reaches a maximum surface concentration plateau typical of Langmuir adsorption. At this point, increasing the fibrinogen solution concentration does not affect the amount of fibrinogen adsorbed to the CPAC at equilibrium. The linearized form of this isotherm (Figure 8B) allows the calculation of the maximum surface concentration, Γ_{max}, the binding affinity constant, K, and $\Delta G°_{ads}$ values, which are summarized for each biomolecule along with the fit of their respective linearized Langmuir models in Table 1.

Table 1: Table of adsorption parameters calculated from linearized Langmuir isotherms

Adsorbate	***MW*** **(g/mol)**	Γ_{max} **(mol/cm^2)**	***K*** **(M^{-1})**	$\Delta G°_{ads}$ **(kJ/mol)**	R^2
Fibrinogen	340000	4.6×10^{-12}	2.2×10^{8}	-56.9	0.999
Albumin	66000	1.2×10^{-11}	2.4×10^{6}	-45.9	0.995
AAG	40800	1.8×10^{-11}	1.5×10^{6}	-44.7	0.994
ELPS	10000	1.4×10^{-10}	5.2×10^{6}	-47.8	0.998
Rhamnolipids	626*	1.6×10^{-9}	5.7×10^{5}	-42.3	0.986

*A weighted average molecular weight of mono and di-rhamnolipids is assumed [23]

Note: Adsorption parameters could not be evaluated for PLPS because no equilibrium adsorption was reached.

A comparison of the maximum surface concentrations of the five adsorbates shows that as the molecular weight of the biomolecule increases, the maximum surface concentration decreases, which is generally to be expected based on steric considerations. The apparent binding affinities for HSA, AAG, and rhamnolipids to CPAC are in the same range as literature values reported for other protein binding interactions measured using the QCM-D [90] and reported protein-drug binding affinities [94, 95]. In contrast, the binding affinity of fibrinogen is considerably higher and is closer to the binding affinity for an antigen-antibody complex [96]. The apparent binding affinity of ELPS for CPAC is nearly 4 times larger than the reported value of about 1.43×10^{6} M^{-1} [33]; however, the LPS molecules are not necessarily comparable as they are from different *E. coli* serotypes [15].

Finally, the negative $\Delta G°_{ads}$ values calculated from the isotherms thermodynamically confirm the spontaneous binding of all of the biomolecules to the CPAC as is observed in the QCM experiments. While not expected to be identical to those in literature due to the different conditions and surfaces used, the $\Delta G°_{ads}$ values of -45.9 kJmol^{-1} and -56.9 kJmol^{-1} reported in this study for HSA and fibrinogen, respectively, are comparable to the range of -48 to -59 kJmol^{-1} reported for BSA and -40 to -55 kJmol^{-1} reported for fibrinogen [92]. Moreover,

the general trend of smaller proteins having a less negative $\Delta G°_{ads}$ value, (i.e., a lower affinity for the surface), than larger proteins, is also observed in this study [92].

The spontaneous binding between the serum proteins and CPAC, particularly the strong affinity with fibrinogen, could limit bioavailability of CPAC in the urinary tract. This is a factor that should be taken into account when determining magnitude and frequency of dose for any future clinical trials involving the use of CPAC to prevent recurrent UTIs. Furthermore, the spontaneous binding of rhamnolipids from *P. aeruginosa* to CPAC supports the hypothesis that CPAC could affect *P. aeruginosa* motility by interacting with the rhamnolipids [30]. However, the difference of an order of magnitude in the binding affinities of LPS from *E. coli* and rhamnolipids from *P. aeruginosa*, and the vastly different time-dependent binding behaviours of the different bacterial components to the CPAC, suggest that CPAC acts to prevent infections via different mechanisms and potentially with different effectiveness depending on the bacterium, another factor that should be taken into account before prescribing CPAC as a preventative measure against recurrent UTIs.

In this study, we confirm that QCM-D can be used to directly investigate the interactions between CPAC and biomolecules in real-time. Moreover, we demonstrate that CPAC binding to human serum proteins is a potential limitation to the bioavailability of CPAC in the urinary tract and that CPAC plays an interfering role against the bacterial virulence factors LPS and rhamnolipids. Because individual binding affinities do not always reflect the outcome of competitive binding studies, additional research should investigate the time-dependent competitive binding of the biomolecules to build upon the results presented here and provide additional clarity on the bioavailability and the mechanisms by which cranberry prevents bacterial infection.

2.4 Acknowledgments

This research was financially supported by NSERC, the CRC Program, the Cranberry Institute, and the Wisconsin Cranberry Board. The authors would like to acknowledge A.B. Howell (Rutgers) for providing cranberry derived proanthocyanidins, Andreas Wargenau for assistance with Langmuir isotherms, and Ché O'May for assistance with manuscript revision.

Chapter 3: Conclusion and Suggested Future Work

This thesis presents the results of experiments conducted using the QCM-D to directly investigate the interactions between CPAC and human serum proteins or bacterial components (LPS and rhamnolipid). While all of the molecules spontaneously bind to the CPAC, CPAC was found to have the strongest affinity with fibrinogen, which could limit bioavailability of the CPAC in the urinary tract. However, CPAC was also found to bind to the other molecules with varying degrees of affinity. Because individual binding affinities do not always reflect the outcome of competitive binding studies, future experiments should investigate the time-dependent competitive binding of the biomolecules from mixtures containing physiologically relevant biomolecule concentrations. The results of competitive binding experiments are particularly important for the proteins, as the particular protein that drugs are bound to in serum can influence drug interactions. In addition to competitive binding experiments in phosphate buffered saline, a very controlled environment, it would be of interest to perform binding experiments in complex media that is more representative of real conditions, for example in serum or in urine.

Because LPS from *E. coli*, as well as rhamnolipids and LPS from *P. aeruginosa* all bind to the CPAC, albeit with vastly different time dependent binding behaviour, it is likely that CPAC acts to prevent infections via different mechanisms and potentially with different effectiveness depending on the bacteria. It would be interesting in the future to correlate the binding results for the molecular LPS from different bacteria serotypes to studies researching the binding of whole bacteria to CPAC. As certain bacteria can express a variety of LPS molecules, bacteria mutants capable of expressing only one particular form of LPS can be used to elucidate which elements of the LPS are most important for bacteria-CPAC interactions.

The binding of other molecules implicated in CPAC bioactivity could be researched using QCM-D to further elucidate the mechanism via which cranberry acts to prevent bacterial infections. Other molecules of interest include molecules present in the urine, cell surface proteins and molecules associated with human epithelial cells in the urinary tract, and other bacterial components involved in motility and adhesion beyond LPS and rhamnolipids. While the purification of proteins, molecules, and macromolecular structures such as cell membrane proteins from human cells or fimbriae and flagella from bacteria may be challenging, the information regarding the potential mechanisms of action of CPAC would be invaluable.

Finally, while investigations into molecular binding interactions are necessary to determine mechanisms of cranberry action, further *in vivo* studies into the metabolism and bioavailability of cranberry are essential. From the moment of ingestion until it reaches the site of action, cranberry encounters a plethora of proteins, molecules, and enzymes in the gastrointestinal tract, the bloodstream, and in the urinary tract itself. Thus a much more thorough understanding of the *in vivo* metabolic pathway of cranberry and its derivatives is needed in order for cranberry to become a widely accepted method of preventing UTIs.

References

[1] L. E. Nicolle, "Update in adult urinary tract infection," *Current Infectious Disease Reports,* vol. 13, pp. 552-560, 2011.

[2] R. Niska*, et al.*, "National hospital ambulatory medical care survey: 2007 emergency department summary," *National Health Statistics Reports,* vol. 26, pp. 1-31, 2010.

[3] G. R. Nielubowicz and H. L. Mobley, "Host–pathogen interactions in urinary tract infection," *Nature Reviews Urology,* vol. 7, pp. 430-441, 2010.

[4] A. E. Barber*, et al.*, "Urinary tract infections: current and emerging management strategies," *Clinical Infectious Diseases,* 2013.

[5] C. Svanborg and G. Godaly, "Bacterial virulence in urinary tract infection," *Infectious Disease Clinics of North America,* vol. 11, pp. 513-529, 1997.

[6] G. Reid and J. D. Sobel, "Bacterial adherence in the pathogenesis of urinary tract infection: a review," *Review of Infectious Diseases,* vol. 9, pp. 470-487, 1987.

[7] M. C. Lane*, et al.*, "Role of motility in the colonization of uropathogenic *Escherichia coli* in the urinary tract," *Infection and Immunity,* vol. 73, pp. 7644-7656, 2005.

[8] M. Lane and H. Mobley, "Role of P-fimbrial-mediated adherence in pyelonephritis and persistence of uropathogenic *Escherichia coli* (UPEC) in the mammalian kidney," *Kidney International,* vol. 72, pp. 19-25, 2007.

[9] I. Connell*, et al.*, "Type 1 fimbrial expression enhances *Escherichia coli* virulence for the urinary tract," *Proceedings of the National Academy of Sciences,* vol. 93, pp. 9827-9832, 1996.

[10] F. K. Bahrani-Mougeot*, et al.*, "Type 1 fimbriae and extracellular polysaccharides are preeminent uropathogenic *Escherichia coli* virulence determinants in the murine urinary tract," *Molecular Microbiology,* vol. 45, pp. 1079-1093, 2002.

[11] M. Lane*, et al.*, "Expression of flagella is coincident with uropathogenic *Escherichia coli* ascension to the upper urinary tract," *Proceedings of the National Academy of Sciences,* vol. 104, pp. 16669-16674, 2007.

[12] K. J. Wright*, et al.*, "Uropathogenic *Escherichia coli* flagella aid in efficient urinary tract colonization," *Infection and Immunity,* vol. 73, pp. 7657-7668, 2005.

[13] T. Lindhout*, et al.*, "Truncation in the core oligosaccharide of lipopolysaccharide affects flagella-mediated motility in *Pseudomonas aeruginosa* PAO1 via modulation of cell surface attachment," *Microbiology,* vol. 155, pp. 3449-3460, 2009.

[14] C. Alexander and E. T. Rietschel, "Invited review: bacterial lipopolysaccharides and innate immunity," *Journal of Endotoxin Research,* vol. 7, pp. 167-202, 2001.

[15] C. Erridge*, et al.*, "Structure and function of lipopolysaccharides," *Microbes and Infection,* vol. 4, pp. 837-851, 2002.

[16] B. A. Jucker*, et al.*, "Quantification of polymer interactions in bacterial adhesion," *Environmental Science & Technology,* vol. 32, pp. 2909-2915, 1998.

[17] Y. A. Knirel*, et al.*, "Review: Conserved and variable structural features in the lipopolysaccharide of *Pseudomonas aeruginosa*," *Journal of Endotoxin Research,* vol. 12, pp. 324-336, 2006.

[18] G. Soberón-Chávez*, et al.*, "Production of rhamnolipids by *Pseudomonas aeruginosa*," *Applied Microbiology and Biotechnology,* vol. 68, pp. 718-725, 2005.

[19] L. Zulianello*, et al.*, "Rhamnolipids are virulence factors that promote early infiltration of primary human airway epithelia by *Pseudomonas aeruginosa*," *Infection and Immunity,* vol. 74, pp. 3134-3147, 2006.

[20] J. P. Pearson*, et al.*, "Roles of *Pseudomonas aeruginosa las* and *rhl* quorum-sensing systems in control of elastase and rhamnolipid biosynthesis genes," *Journal of Bacteriology,* vol. 179, pp. 5756-5767, 1997.

[21] R. Kumar*, et al.*, "Quorum sensing is necessary for the virulence of *Pseudomonas aeruginosa* during urinary tract infection," *Kidney International,* vol. 76, pp. 286-292, 2009.

[22] N. C. Caiazza*, et al.*, "Rhamnolipids modulate swarming motility patterns of *Pseudomonas aeruginosa*," *Journal of Bacteriology,* vol. 187, pp. 7351-7361, 2005.

[23] A. M. Abdel-Mawgoud*, et al.*, "Rhamnolipids: diversity of structures, microbial origins and roles," *Applied Microbiology and Biotechnology,* vol. 86, pp. 1323-1336, 2010.

[24] L. Dethlefsen*, et al.*, "The pervasive effects of an antibiotic on the human gut microbiota, as revealed by deep 16S rRNA sequencing," *PLoS Biology,* vol. 6, p. e280, 2008.

[25] M. A. J. Beerepoot*, et al.*, "Cranberries vs antibiotics to prevent urinary tract infections: a randomized double-blind noninferiority trial in premenopausal women," *Archives of Internal Medicine,* vol. 171, p. 1270, 2011.

[26] P. Cos*, et al.*, "Proanthocyanidins in health care: current and new trends," *Current Medicinal Chemistry,* vol. 11, pp. 1345-1359, 2004.

[27] A. B. Howell, "Bioactive compounds in cranberries and their role in prevention of urinary tract infections," *Molecular Nutrition & Food Research,* vol. 51, pp. 732-737, 2007.

[28] I. A. Eydelnant and N. Tufenkji, "Cranberry derived proanthocyanidins reduce bacterial adhesion to selected biomaterials," *Langmuir,* vol. 24, pp. 10273-10281, 2008.

[29] J. Côté*, et al.*, "Bioactive compounds in cranberries and their biological properties," *Critical Reviews in Food Science and Nutrition,* vol. 50, pp. 666-679, 2010.

[30] C. O'May and N. Tufenkji, "*Pseudomonas aeruginosa* swarming motility is blocked by cranberry proanthocyanidins and other tannin-containing materials," *Applied and Environmental Microbiology,* pp. AEM. 02677-10v1, 2011.

[31] L. Y. Foo*, et al.*, "The structure of cranberry proanthocyanidins which inhibit adherence of uropathogenic P-fimbriated *Escherichia coli in vitro*," *Phytochemistry,* vol. 54, pp. 173-181, 2000.

[32] C. C. Neto, "Cranberry and its phytochemicals: a review of *in vitro* anticancer studies," *The Journal of Nutrition,* vol. 137, p. 186S, 2007.

[33] J. B. Delehanty*, et al.*, "Binding and neutralization of lipopolysaccharides by plant proanthocyanidins," *Journal of Natural Products,* vol. 70, pp. 1718-1724, 2007.

[34] N. Blatherwick, "The specific role of foods in relation to the composition of the urine," *Archives of Internal Medicine,* vol. 14, p. 409, 1914.

[35] M. B. Habash*, et al.*, "The effect of water, ascorbic acid, and cranberry derived supplementation on human urine and uropathogen adhesion to silicone rubber," *Canadian Journal of Microbiology,* vol. 45, pp. 691-694, 1999.

[36] K. Valentová*, et al.*, "Biosafety, antioxidant status, and metabolites in urine after consumption of dried cranberry juice in healthy women: a pilot double-blind placebo-controlled trial," *Journal of Agricultural and Food Chemistry,* vol. 55, pp. 3217-3224, 2007.

[37] I. Ofek*, et al.*, "Anti-*Escherichia coli* adhesin activity of cranberry and blueberry juices," *New England Journal of Medicine,* vol. 324, pp. 1599-1599, 1991.

[38] M. Habash*, et al.*, "Adsorption of urinary components influences the zeta potential of uropathogen surfaces," *Colloids and Surfaces B: Biointerfaces,* vol. 19, pp. 13-17, 2000.

[39] Y. Liu*, et al.*, "Cranberry changes the physicochemical surface properties of *E. coli* and adhesion with uroepithelial cells," *Colloids and Surfaces B: Biointerfaces,* vol. 65, pp. 35-42, 2008.

[40] S. Ahuja*, et al.*, "Loss of fimbrial adhesion with the addition of *Vaccinum macrocarpon* to the growth medium of P-fimbriated *Escherchia coli*," *The Journal of Urology,* vol. 159, pp. 559-562, 1998.

[41] L. Y. Foo*, et al.*, "A-type proanthocyanidin trimers from cranberry that inhibit adherence of uropathogenic P-fimbriated *Escherichia coli*," *Journal of Natural Products,* vol. 63, pp. 1225-1228, 2000.

[42] K. Harmidy*, et al.*, "Perturbation of host cell cytoskeleton by cranberry proanthocyanidins and their effect on enteric infections," *PLoS ONE,* vol. 6, p. e27267, 2011.

[43] D. Allison*, et al.*, "Influence of cranberry juice on attachment of *Escherichia coli* to glass," *Journal of Basic Microbiology,* vol. 40, pp. 3-6, 2000.

[44] B. Johnson-White*, et al.*, "Prevention of nonspecific bacterial cell adhesion in immunoassays by use of cranberry juice," *Analytical Chemistry,* vol. 78, pp. 853-857, 2006.

[45] K. Gupta*, et al.*, "Cranberry products inhibit adherence of p-fimbriated *Escherichia coli* to primary cultured bladder and vaginal epithelial cells," *The Journal of Urology,* vol. 177, pp. 2357-2360, 2007.

[46] Y. Tao*, et al.*, "Oral consumption of cranberry juice cocktail inhibits molecular-scale adhesion of clinical uropathogenic *Escherichia coli*," *Journal of Medicinal Food,* vol. 14, pp. 739-745, 2011.

[47] P. Di Martino*, et al.*, "Reduction of *Escherichia coli* adherence to uroepithelial bladder cells after consumption of cranberry juice: a double-blind randomized placebo-controlled cross-over trial," *World Journal of Urology,* vol. 24, pp. 21-27, 2006.

[48] G. Hidalgo*, et al.*, "Inhibition of *Escherichia coli* CFT073 fliC expression and motility by cranberry materials," *Applied and Environmental Microbiology,* vol. 77, pp. 6852-6857, 2011.

[49] J. McCall*, et al.*, "Cranberry impairs selected behaviours essential for virulence in *Proteus mirabilis* HI4320," *Canadian Journal of Microbiology,* vol. 59, 2013.

[50] G. Hidalgo*, et al.*, "Induction of a state of iron limitation in uropathogenic *Escherichia coli* CFT073 by cranberry-derived proanthocyanidins as revealed by microarray analysis," *Applied and Environmental Microbiology,* vol. 77, pp. 1532-1535, 2011.

[51] T. Kontiokari*, et al.*, "Randomised trial of cranberry-lingonberry juice and Lactobacillus GG drink for the prevention of urinary tract infections in women," *BMJ,* vol. 322, p. 1571, 2001.

[52] C. Barbosa-Cesnik*, et al.*, "Cranberry juice fails to prevent recurrent urinary tract infection: results from a randomized placebo-controlled trial," *Clinical Infectious Diseases,* vol. 52, pp. 23-30, 2011.

[53] J. Serrano*, et al.*, "Tannins: current knowledge of food sources, intake, bioavailability and biological effects," *Molecular Nutrition & Food Research,* vol. 53, pp. S310-S329, 2009.

[54] M. Hisano*, et al.*, "Cranberries and lower urinary tract infection prevention," *Clinics,* vol. 67, pp. 661-668, 2012.

[55] M.-P. Gonthier*, et al.*, "Metabolism of dietary procyanidins in rats," *Free Radical Biology and Medicine,* vol. 35, pp. 837-844, 2003.

[56] C. Santos-Buelga and A. Scalbert, "Proanthocyanidins and tannin-like compounds–nature, occurrence, dietary intake and effects on nutrition and health," *Journal of the Science of Food and Agriculture,* vol. 80, pp. 1094-1117, 2000.

[57] N. A. Kratochwil*, et al.*, "Predicting plasma protein binding of drugs: a new approach," *Biochemical Pharmacology,* vol. 64, pp. 1355-1374, 2002.

[58] A. E. Hagerman and L. G. Butler, "The specificity of proanthocyanidin-protein interactions," *Journal of Biological Chemistry,* vol. 256, pp. 4494-4497, 1981.

[59] W. E. Artz*, et al.*, "Interaction of synthetic proanthocyanidin dimer and trimer with bovine serum albumin and purified bean globulin fraction G-1," *Journal of Agricultural and Food Chemistry,* vol. 35, pp. 417-421, 1987.

[60] A. J. Charlton*, et al.*, "Tannin interactions with a full-length human salivary proline-rich protein display a stronger affinity than with single proline-rich repeats," *FEBS Letters,* vol. 382, pp. 289-292, 1996.

[61] A. Janshoff and C. Steinem, "Quartz crystal microbalance for bioanalytical applications," *Sensors Update,* vol. 9, pp. 313-354, 2001.

[62] M. C. Dixon, "Quartz crystal microbalance with dissipation monitoring: enabling real-time characterization of biological materials and their interactions," *Journal of Biomolecular Techniques,* vol. 19, p. 151, 2008.

[63] B. Becker and M. A. Cooper, "A survey of the 2006–2009 quartz crystal microbalance biosensor literature," *Journal of Molecular Recognition,* vol. 24, pp. 754-787, 2011.

[64] G. Sauerbrey, "Verwendung von Schwingquarzen zur Wägung dünner Schichten und zur Mikrowägung," *Zeitschrift für Physik A Hadrons and Nuclei,* vol. 155, pp. 206-222, 1959.

[65] W. H. King Jr, "Piezoelectric Sorption Detector," *Analytical Chemistry,* vol. 36, pp. 1735-1739, 1964.

[66] C. O'Sullivan and G. Guilbault, "Commercial quartz crystal microbalances-theory and applications," *Biosensors and Bioelectronics,* vol. 14, pp. 663-670, 1999.

[67] T. Nomura and M. Okuhara, "Frequency shifts of piezoelectric quartz crystals immersed in organic liquids," *Analytica Chimica Acta,* vol. 142, pp. 281-284, 1982.

[68] K. K. Kanazawa and J. G. Gordon, "Frequency of a quartz microbalance in contact with liquid," *Analytical Chemistry,* vol. 57, pp. 1770-1771, 1985.

[69] S. J. Martin*, et al.*, "Characterization of a quartz crystal microbalance with simultaneous mass and liquid loading," *Analytical Chemistry,* vol. 63, pp. 2272-2281, 1991.

[70] M. Rodahl*, et al.*, "Quartz crystal microbalance setup for frequency and Q-factor measurements in gaseous and liquid environments," *Review of Scientific Instruments,* vol. 66, pp. 3924-3930, 1995.

[71] F. Höök*, et al.*, "Structural changes in hemoglobin during adsorption to solid surfaces: effects of pH, ionic strength, and ligand binding," *Proceedings of the National Academy of Sciences,* vol. 95, pp. 12271-12276, 1998.

[72] F. Höök*, et al.*, "Measurements using the quartz crystal microbalance technique of ferritin monolayers on methyl-thiolated gold: dependence of energy dissipation and saturation coverage on salt concentration," *Journal of Colloid and Interface Science,* vol. 208, pp. 63-67, 1998.

[73] N. Ishida and S. Biggs, "Direct observation of the phase transition for a poly (N-isopropylacryamide) layer grafted onto a solid surface by AFM and QCM-D," *Langmuir,* vol. 23, pp. 11083-11088, 2007.

[74] S. Chernyy*, et al.*, "Elucidation of the mechanism of surface-initiated atom transfer radical polymerization from a diazonium-based initiator layer," *Journal of Polymer Science Part A: Polymer Chemistry,* vol. 50, pp. 4465-4475, 2012.

[75] F. Höök*, et al.*, "Variations in coupled water, viscoelastic properties, and film thickness of a Mefp-1 protein film during adsorption and cross-linking: a quartz crystal microbalance with dissipation monitoring, ellipsometry, and surface plasmon resonance study," *Analytical Chemistry,* vol. 73, pp. 5796-5804, 2001.

[76] M. Andersson*, et al.*, "Quartz crystal microbalance-with dissipation monitoring (QCM-D) for real time measurements of blood coagulation density and immune complement activation on artificial surfaces," *Biosensors and Bioelectronics,* vol. 21, pp. 79-86, 2005.

[77] A. Tsortos*, et al.*, "Shear acoustic wave biosensor for detecting DNA intrinsic viscosity and conformation: A study with QCM-D," *Biosensors and Bioelectronics,* vol. 24, pp. 836-841, 2008.

[78] R. J. Rawle*, et al.*, "A real-time QCM-D approach to monitoring mammalian DNA damage using DNA adsorbed to a polyelectrolyte surface," *Biomacromolecules,* vol. 9, pp. 9-12, 2007.

[79] K. Min*, et al.*, "A simple and direct electrochemical detection of interferon-[gamma] using its RNA and DNA aptamers," *Biosensors and Bioelectronics,* vol. 23, pp. 1819-1824, 2008.

[80] N. Weber*, et al.*, "Viscoelastic properties of fibrinogen adsorbed to the surface of biomaterials used in blood-contacting medical devices," *Langmuir,* vol. 23, pp. 3298-3304, 2007.

[81] A. Reisch*, et al.*, "Polyelectrolyte multilayers capped with polyelectrolytes bearing phosphorylcholine and triethylene glycol groups: parameters influencing antifouling properties," *Langmuir,* vol. 25, pp. 3610-3617, 2009.

[82] S. Volden*, et al.*, "Use of cellulose derivatives on gold surfaces for reduced nonspecific adsorption of immunoglobulin G," *Colloids and Surfaces B: Biointerfaces,* vol. 72, pp. 266-271, 2009.

[83] M. Berglin*, et al.*, "Fibrinogen adsorption and conformational change on model polymers: novel aspects of mutual molecular rearrangement," *Langmuir,* vol. 25, pp. 5602-5608, 2009.

[84] F. Höök*, et al.*, "A comparative study of protein adsorption on titanium oxide surfaces using in situ ellipsometry, optical waveguide lightmode spectroscopy, and quartz crystal microbalance/dissipation," *Colloids and Surfaces B: Biointerfaces,* vol. 24, pp. 155-170, 2002.

[85] C. Ayela*, et al.*, "Antibody-antigenic peptide interactions monitored by SPR and QCM-D: A model for SPR detection of IA-2 autoantibodies in human serum," *Biosensors and Bioelectronics,* vol. 22, pp. 3113-3119, 2007.

[86] F. Höök*, et al.*, "Energy dissipation kinetics for protein and antibody-antigen adsorption under shear oscillation on a quartz crystal microbalance," *Langmuir,* vol. 14, pp. 729-734, 1998.

[87] S. D. Carrigan*, et al.*, "Real-time QCM-D immunoassay through oriented antibody immobilization using cross-linked hydrogel biointerfaces," *Langmuir,* vol. 21, pp. 5966-5973, 2005.

[88] C. A. Aurell and A. O. Wistrom, "Critical aggregation concentrations of gram-negative bacterial lipopolysaccharides (LPS)," *Biochemical and Biophysical Research Communications,* vol. 253, pp. 119-123, 1998.

[89] J. Malmström*, et al.*, "Viscoelastic modeling of highly hydrated laminin layers at homogeneous and nanostructured surfaces: quantification of protein layer properties using QCM-D and SPR," *Langmuir,* vol. 23, pp. 9760-9768, 2007.

[90] S. H. Brewer*, et al.*, "Probing BSA binding to citrate-coated gold nanoparticles and surfaces," *Langmuir,* vol. 21, pp. 9303-9307, 2005.

[91] I. Reviakine*, et al.*, "Hearing what you cannot see and visualizing what you hear: Interpreting quartz crystal microbalance data from solvated interfaces," *Analytical Chemistry,* vol. 83, pp. 8838-8848, 2011.

[92] N. P. Cosman and S. G. Roscoe, "Electrochemical quartz crystal nanobalance (EQCN) studies of protein interfacial behavior at Pt," *Langmuir,* vol. 20, pp. 1711-1720, 2004.

[93] N. Samadi*, et al.*, "Structural characterization and surface activities of biogenic rhamnolipid surfactants from *Pseudomonas aeruginosa* isolate MN1 and synergistic effects against methicillin-resistant *Staphylococcus aureus*," *Folia Microbiologica,* vol. 57, pp. 501-508, 2012.

[94] H. Xuan and D. S. Hage, "Immobilization of α< sub> 1</sub>-acid glycoprotein for chromatographic studies of drug–protein binding," *Analytical biochemistry,* vol. 346, pp. 300-310, 2005.

[95] Å. Frostell-Karlsson*, et al.*, "Biosensor analysis of the interaction between immobilized human serum albumin and drug compounds for prediction of human serum albumin binding levels," *Journal of medicinal chemistry,* vol. 43, pp. 1986-1992, 2000.

[96] J. Piehler*, et al.*, "Assessment of affinity constants by rapid solid phase detection of equilibrium binding in a flow system," *Journal of Immunological Methods,* vol. 201, pp. 189-206, 1997.

[97] O. Westphal and K. Jann, "Bacterial lipopolysaccharides: Extraction with phenol-water and further applications of the procedure," *Methods in Carbohydrate Chemistry,* vol. 5, pp. 83-91, 1965.

Appendix 1: Effect of the Purity of *E. coli* LPS

LPS from *E. coli* serotype O111:B4 can be purchased from Sigma-Aldrich at multiple purities. One of the basic methods of LPS extraction is phenol extraction [97], however this leaves a product with low purity (Sigma Product Sheet, L2630). This product can then be further purified using gel filtration chromatography and ion exchange chromatography. The amount of protein impurities, the amount of RNA impurities, and the cost of each additional purification method for the ELPS are summarized in Table 2.

Table 2: A comparison of the various purities and associated costs of LPS available for purchase

	Purity	**Cost**
Phenol Extraction	Protein <1-3% RNA up to 60%	$85
Gel Filtration Chromatography	Protein <1-3% RNA 10-20%	$259
Ion Exchange Chromatography	Protein <1% RNA <1%	$295

LPS isolated by phenol extraction was used for initial adsorption experiments and then the results were compared to those achieved using higher purity LPS. A concern in the initial experiments was that impurities were binding to the CPAC layer and causing the frequency shift rather than the ELPS binding to the CPAC. Thus, the binding isotherms for low purity (phenol extraction) and high purity (ion exchange) ELPS were constructed and compared in order to test the contribution of protein or RNA impurities binding to the CPAC.

The phenol extracted ELPS and the ion exchange chromatography ELPS did bind in different quantities but did not change the overall binding behaviour of the molecule with the CPAC (Figure 9).

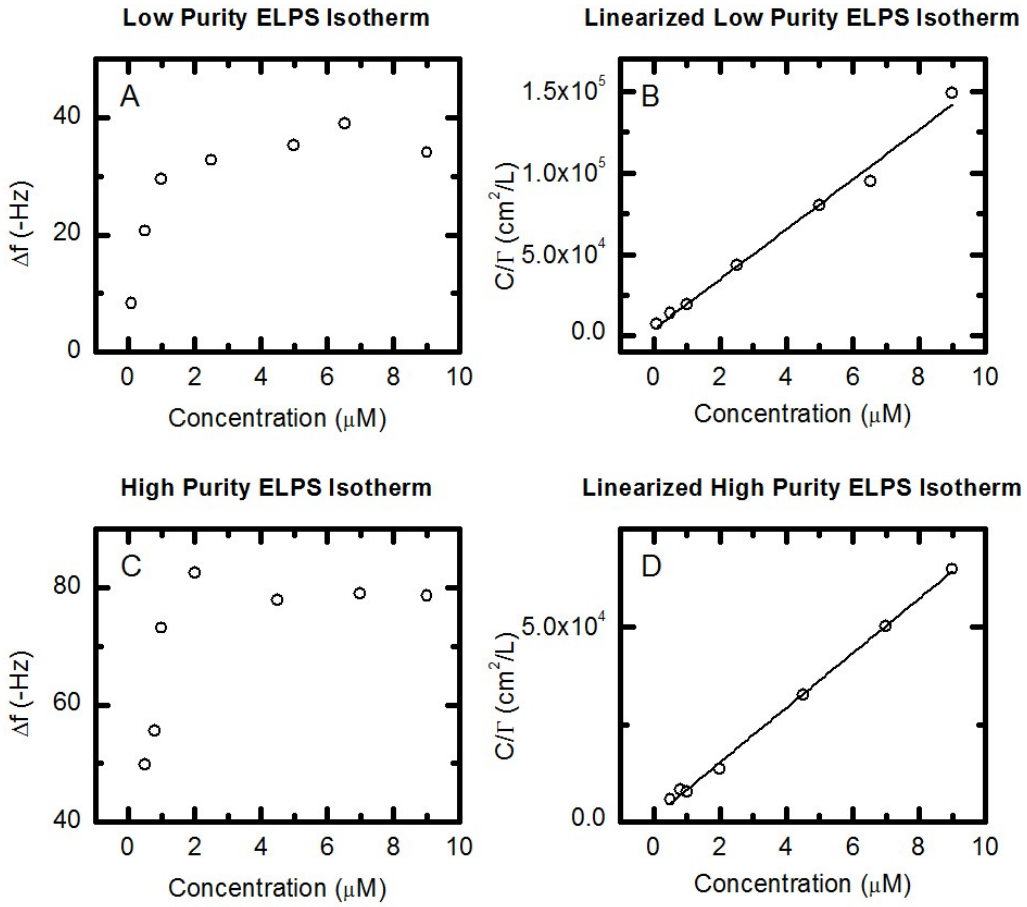

Figure 9: The isotherms and the linearized Langmuir isotherms for (A-B) low purity phenol extracted ELPS and (C-D) high purity ion exchange ELPS.

The low purity (phenol extraction) and high purity (ion exchange) ELPS are both well described by the Langmuir adsorption model, however the magnitude of the frequency shift is much larger, almost twice as large, for the higher purity ELPS. Similarly the maximum surface coverage and the apparent binding constant are larger for the high purity ELPS. These differences could be because at the low purity, small fragments of RNA or protein impurities are binding to the CPAC and preventing the much larger LPS molecules from binding to those sites. Regardless, the results show that high purity LPS must be used for binding studies with CPAC or other molecules that potentially bind to sample impurities.

Appendix 2: Linearized Isotherms

The linearized Langmuir isotherms used to calculate the adsorption parameters listed in Table 1 can be seen in the figures below.

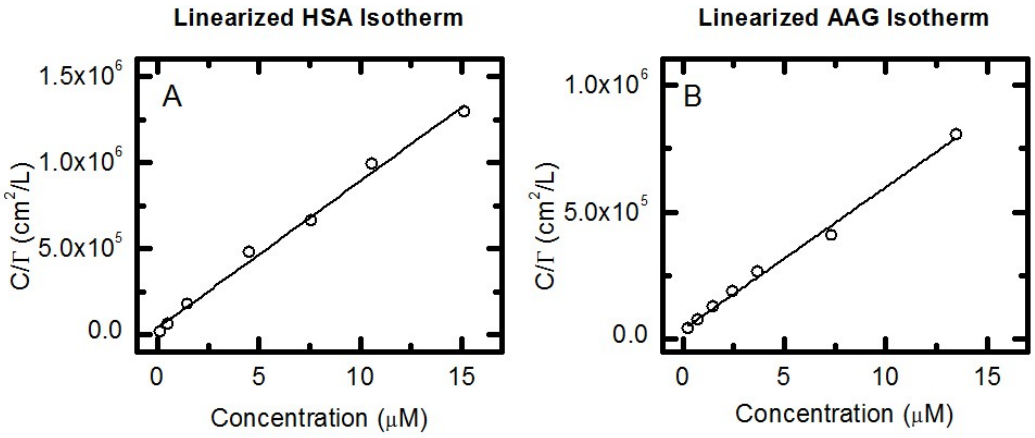

Figure 10: The linearized Langmuir isotherms for the proteins (A) HSA and (B) AAG.

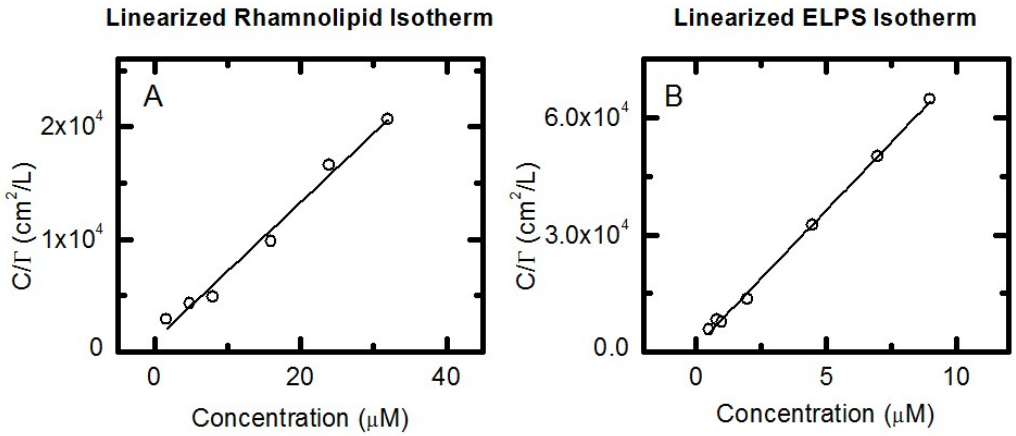

Figure 11: The linearized Langmuir isotherms for the (A) rhamnolipids and the (B) ELPS.